

First Search for Dyons with the Full MoEDAL Trapping Detector in 13 TeV *pp* Collisions

B. Acharya,^{1,‡} J. Alexandre,¹ P. Benes,² B. Bergmann,² J. Bernabéu,³ A. Bevan,⁴ H. Branzas,⁵ P. Burian,² M. Campbell,⁶ S. Cecchini,⁷ Y. M. Cho,⁸ M. de Montigny,⁹ A. De Roeck,⁶ J. R. Ellis,^{1,10,§} M. El Sawy,^{6,||} M. Fairbairn,¹ D. Felea,⁵ M. Frank,¹¹ J. Hays,⁴ A. M. Hirt,¹² J. Janecek,² M. Kalliokoski,¹³ A. Korzenev,¹⁴ D. H. Lacarrère,⁶ C. Leroy,¹⁵ G. Levi,¹⁶ A. Lioni,¹⁴ J. Mamuzic,³ A. Maulik,^{7,9} A. Margiotta,¹⁶ N. Mauri,⁷ N. E. Mavromatos,¹ P. Mermod,^{14,*} M. Mieskolainen,¹³ L. Millward,⁴ V. A. Mitsou,³ R. Orava,¹³ I. Ostrovskiy,¹⁷ P.-P. Ouimet,^{9,¶} J. Papavassiliou,³ B. Parker,¹⁸ L. Patrizii,⁷ G. E. Pávlas,⁵ J. L. Pinfold,^{9,†} L. A. Popa,⁵ V. Popa,⁵ M. Pozzato,⁷ S. Pospisil,² A. Rajantie,¹⁹ R. Ruiz de Austri,³ Z. Sahnoun,^{7,**} M. Sakellariadou,¹ A. Santra,³ S. Sarkar,¹ G. Semenoff,²⁰ A. Shaa,⁹ G. Sirri,⁷ K. Sliwa,²¹ R. Soluk,⁹ M. Spurio,¹⁶ M. Staelens,⁹ M. Suk,² M. Tenti,²² V. Togo,⁷ J. A. Tuszyński,⁹ A. Upreti,¹⁷ V. Vento,³ O. Vives,³ and A. Wall¹⁷

(MoEDAL Collaboration)

¹*Theoretical Particle Physics and Cosmology Group, Physics Department, King's College, London, United Kingdom*²*IEAP, Czech Technical University in Prague, Prague, Czech Republic*³*IFIC, Universitat de València—CSIC, Valencia, Spain*⁴*School of Physics and Astronomy, Queen Mary University of London, London, United Kingdom*⁵*Institute of Space Science, Bucharest, Măgurele, Romania*⁶*Experimental Physics Department, CERN, Geneva, Switzerland*⁷*INFN, Section of Bologna, Bologna, Italy*⁸*Center for Quantum Spacetime, Sogang University, Seoul, Korea*⁹*Physics Department, University of Alberta, Edmonton, Alberta, Canada*¹⁰*Theoretical Physics Department, CERN, Geneva, Switzerland*¹¹*Department of Physics, Concordia University, Montréal, Québec, Canada*¹²*Department of Earth Sciences, Swiss Federal Institute of Technology, Zurich, Switzerland*¹³*Physics Department, University of Helsinki, Helsinki, Finland*¹⁴*Département de Physique Nucléaire et Corpusculaire, Université de Genève, Geneva, Switzerland*¹⁵*Département de Physique, Université de Montréal, Québec, Canada*¹⁶*INFN, Section of Bologna and Department of Physics and Astronomy, University of Bologna, Bologna, Italy*¹⁷*Department of Physics and Astronomy, University of Alabama, Tuscaloosa, Alabama, USA*¹⁸*Institute for Research in Schools, Canterbury, United Kingdom*¹⁹*Department of Physics, Imperial College London, United Kingdom*²⁰*Department of Physics, University of British Columbia, Vancouver, British Columbia, Canada*²¹*Department of Physics and Astronomy, Tufts University, Medford, Massachusetts, USA*²²*INFN, CNAF, Bologna, Italy*

(Received 2 March 2020; revised 10 October 2020; accepted 12 January 2021; published 19 February 2021)

The MoEDAL trapping detector consists of approximately 800 kg of aluminum volumes. It was exposed during run 2 of the LHC program to 6.46 fb^{-1} of 13 TeV proton-proton collisions at the LHCb interaction point. Evidence for dyons (particles with electric and magnetic charge) captured in the trapping detector was sought by passing the aluminum volumes comprising the detector through a superconducting quantum interference device (SQUID) magnetometer. The presence of a trapped dyon would be signaled by a persistent current induced in the SQUID magnetometer. On the basis of a Drell-Yan production model, we exclude dyons with a magnetic charge ranging up to five Dirac charges ($5g_D$) and an electric charge up to 200 times the fundamental electric charge for mass limits in the range 870–3120 GeV and also monopoles with magnetic charge up to and including $5g_D$ with mass limits in the range 870–2040 GeV.

DOI: [10.1103/PhysRevLett.126.071801](https://doi.org/10.1103/PhysRevLett.126.071801)

Published by the American Physical Society under the terms of the [Creative Commons Attribution 4.0 International license](https://creativecommons.org/licenses/by/4.0/). Further distribution of this work must maintain attribution to the author(s) and the published article's title, journal citation, and DOI. Funded by SCOAP³.

The search for the magnetic monopole has been a key concern of fundamental physics since Dirac in 1931 [1] demonstrated its existence was consistent with quantum mechanics provided the quantization condition (in SI units) $g/e = n(c/2\alpha_{em})$ is satisfied, where g is the magnetic

charge, e is a unit electric charge, c is the speed of light, α_{em} is the fine structure constant, and n is an integer. When $n = 1$, then $g = g_D$, one Dirac charge. There is a long history of direct searches for magnetic monopoles at accelerators [2], most recently at the LHC [3–9], and there have also been extensive searches for monopole relics from the early Universe in cosmic rays and in materials [10–12].

The existence of the dyon, a particle with both magnetic and electric charge, was first proposed by Schwinger in 1969 [13]. Schwinger derived the following charge quantization condition by considering the interaction of two dyons:

$$e_1 g_2 - e_2 g_1 = \frac{n}{2} \hbar c, \quad (1)$$

where e_1 and e_2 and g_1 and g_2 are the electric and magnetic charges of the two dyons, respectively. This quantization condition does not, by itself, fix the electric charge of the dyon and provides no *a priori* limitation on the size of the electric charge of the dyon. However, the issue of the charge of the quantum dyon has been studied carefully by semiclassical reasoning [14], and it has been concluded that in CP -conserving theories the dyon charge is quantized as an integer multiple of the fundamental charge, $q = ne$.

When the theory admits CP nonconservation, this is no longer the case. The topologically nontrivial vacuum structure of non-Abelian gauge theories is characterized by the vacuum angle θ , or “theta term,” which can be added to the Lagrangian for Yang-Mills theory without spoiling renormalizability. Witten [15] considered CP violation induced by a vacuum angle in the context of the Georgi-Glashow model that gives rise to the non-Abelian monopole of ’t Hooft and Polyakov, showing that dyons are magnetic monopoles with fractional electric charge. He derived the following relation between the dyon’s electric charge and θ :

$$q = ne - \frac{e\theta}{2\pi}. \quad (2)$$

Experiment has found that CP is only weakly violated. As the deviation of the monopole from integral charge is proportional to the strength of CP violation, one would therefore expect the dyon charge to have almost, but not quite, an integer value.

Since Schwinger’s original work, it has been shown that dyons appear generically in theories with monopoles, specifically in many particle-physics theories including grand unified theories [16], Einstein-Yang-Mills theories [17], Kaluza-Klein theory [18], string theory [19], and M theory [20]. Moreover, a number of theoretical scenarios have been proposed that contain electroweak (EW) dyons and monopoles [21–25] that could be detected at the LHC or the High-Luminosity LHC (HL-LHC) [26]. We note also that the production of such EW dyons and monopoles during the EW phase transition in the early Universe would have major implications for cosmology [21].

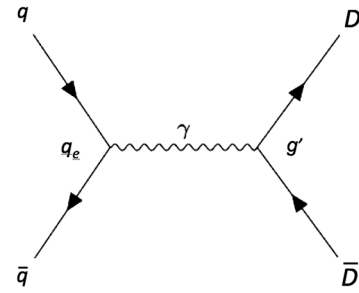


FIG. 1. Feynman-like diagram for dyon-pair direct production at leading order via the benchmark Drell-Yan mechanism. The coupling g' is given by $\sqrt{(g^2 + q^2)}$, in the eikonal approximation that is valid for LHC energies.

The electric charge of a dyon can, in principle, be large. Other suggested examples of highly-electrically-charged (pseudo)stable objects (HECOs) include aggregates of ud - [27] or s -quark matter [28], Q balls [29,30], and the remnants of microscopic black holes [31]. Extensive accelerator searches for HECOs have also been undertaken [8,32,33]. Recently, ATLAS has placed improved limits on HECOs [9], extending a previous excluded charge range from $20 \leq |z| \leq 60$ [8] to $60 \leq |z| \leq 100$ [9], where z is the electric charge [34]. However, we are unaware of any previous accelerator search for dyons.

The Drell-Yan (DY) production mechanism shown in Fig. 1 is frequently employed in accelerator-based searches for monopoles [3–9] and provides a simple benchmark model of monopole-pair production. Here we use a similar DY production model also as a benchmark for dyon production. As in the previous MoEDAL monopole searches [5,6], spins of 0, 1/2, and 1 are considered, and models were generated in MADGRAPH5 [36] using the universal FeynRules output described in Ref. [37]. We used tree-level diagrams and the parton distribution functions NNPDF23 [38] for the DY process. The square of the magnetic charge of the monopole, g^2 , is substituted in the basic DY cross section by $g^2 + q^2$, where q is the electric charge of the dyon defined above. This scaling is in accord with the dual effective theory of Milton and Gamberg [39,40] and the theoretical approach developed for monopoles in Ref. [37] when extended to dyons.

There are two important differences between the signatures of the magnetic monopole and dyon at the LHC that are due to the electric charge of the dyon. First, a relativistic monopole, with magnetic charge ng_D ($n = 1, 2, 3, \dots$) and fractional velocity $\beta = v/c$, where v is the monopole velocity, behaves like an equivalent electric charge $(Ze)_{\text{eq}} = ng_D \beta$, where Z is the effective “atomic number.” The energy loss of a fast monopole is thus very large with a different velocity dependence from that of an electrically charged particle. On the other hand, the ionization energy loss of a dyon is the sum of the energy loss due to its electric

charge and magnetic charge, with their different velocity dependences.

Second, the magnetic monopole follows a curved trajectory in the r - z plane of a solenoidal field, where z is the direction of the field lines and r is the radial dimension, without bending in the transverse plane. This is opposite to the behavior of an electrically charged particle in the same field. On the other hand, the trajectory of a dyon in a solenoidal field curves both in the r - z plane and in the plane transverse to this plane. Thus, its trajectory is distinct from that of either an isolated electric or magnetic charge.

The response of MoEDAL to the passage of a monopole or a dyon differs significantly from those of the general-purpose LHC experiments, ATLAS and CMS. The MoEDAL detector, deployed along with LHCb at LHC intersection point IP8, employs two unconventional passive detection methodologies tuned to the discovery of highly ionizing particles (HIPs). The first, used in this analysis, utilizes a 800 kg trapping detector (MMT) comprised of 2400 aluminum (Al) bars to capture HIPs for further study. The second consists of an array of 186 nuclear track detector stacks. MMT volumes are deployed just upstream and on each side of IP8 in three roughly equal masses each placed 1.0–2.0 m from the IP. After exposure, the MMTs' Al bars are passed through a superconducting quantum interference device (SQUID) magnetometer at the ETH Zurich Laboratory for Natural Magnetism in order to check for the presence of magnetic charge. Further information on the MoEDAL detector is given in Supplemental Material [41], which includes Refs. [42,43].

To date, only the ATLAS and MoEDAL experiments have reported limits on monopole production at the LHC [3–9]. MoEDAL's latest search results [6] include the combined photon-fusion and DY monopole-pair production mechanisms, the former process for the first time at the LHC. Using 4.0 fb^{-1} of data, cross-section upper limits as low as 11 fb were set, and mass limits in the range 1500–3750 GeV were set for magnetic charges up to $5g_D$ for monopoles of spins 0, $1/2$, and 1, the strongest to date at a collider experiment. These limits are based on a *direct* search for magnetic charge, with an unambiguous signature.

The most recent ATLAS search [9] placed 95% confidence level mass limits on DY production of spin-0 and spin- $1/2$ monopoles, with charge $1g_D$, of 1850 and 2370 GeV, respectively. The corresponding ATLAS limits for charge $2g_D$ monopoles are 1725 and 2125 GeV, respectively. For magnetic charge $g_D \leq 2$, these are currently the world's best limits based on the ionizing nature of magnetic monopoles or dyons.

A monopole is expected to be stopped when its velocity falls to $\beta \leq 10^{-3}$ and then bind, due to interaction between the monopole and the nuclear magnetic moment [44–47]. The large magnetic moment gives a predicted monopole-nucleus binding energy (BE) of 0.5–2.5 MeV [44]. These BEs are comparable to the shell model splittings. Thus, it is

reasonable to assume that, in any case, the strong magnetic field in the monopole's vicinity will rearrange the nucleus, allowing it to strongly bind to the nucleus. According to Ref. [44], monopoles with this BE will be bound indefinitely, requiring fields in excess of around 5 T for them to be released. We note in this connection that the MMT volumes are never subjected to such strong magnetic fields.

The dyon is also expected to stop when its velocity falls to $\beta \leq 10^{-3}$. However, the binding of the dyon is complicated by its electric charge. In our analysis, we assume conservatively that only dyons with negative electric charge are bound, since in this case their Coulomb attraction to the positive charge of the nucleus reinforces the interaction between its magnetic charge and the large anomalous nuclear magnetic moment of the aluminum nucleus. Although the trapping condition requires the dyon to be negatively electrically charged, the assumption of DY production of dyon-antidyon pairs implies indirect sensitivity to positively charged dyons at the same level.

A magnetic charge captured in a trapping volume bar is identified and measured as a persistent current in the coil of the SQUID surrounding the transport axis of the MMTs' Al bars. The magnetic pole strength, expressed in units of the Dirac charge, contained in a sample is calculated as $P = C \cdot [(I_2 - I_1) - (I_2^{\text{tray}} - I_1^{\text{tray}})]$, where C is the calibration constant; (I_1) and (I_2) are the currents measured, respectively, before and after the sample has passed through the sensing coil; and I_2^{tray} and I_1^{tray} are the corresponding contributions measured with an empty tray. The empty tray contributions arise from small seemingly random fluctuations of the SQUID measurement due largely to less than perfect grounding of the SQUID magnetometer electronics. It should be noted that the small tray is constructed from G10, a nonmetallic and nonmagnetic fiberglass-epoxy composite that cannot shield or enhance the magnetic signal.

The magnetometer response is calibrated using two independent methods, described in more detail in Ref. [48]. The two methods agree within 10%, which we take as the calibration uncertainty in the pole strength. The magnetometer response is measured to be linear and charge symmetric in a range corresponding to 0.3–300 g_D . During run 2, the plateau value of the calibration dipole sample was remeasured regularly and found to be stable to within less than 1%. In 2018, the SQUID was overhauled, the main improvement being better grounding throughout the SQUID magnetometer mechanics and electronics. This had the effect of substantially reducing fluctuations in the recorded magnetometer values.

Each MMT sample was scanned at least twice. A sample containing a dyon would repeatedly and consistently yield the same nonzero measurements corresponding to the magnetic charge of the dyon. When a dyon is not present, values consistent with zero would be recorded. If the measured pole strength of a sample differed from zero by more than $0.4g_D$ in either of the two initial measurements, it

was considered a candidate. In this way, the probability of false negatives was significantly reduced. A total of 87 candidates were thus identified in data taken in 2015, 2016, and 2017, corresponding to 4.0 fb^{-1} . Only 29 candidates were observed in the data 2018 data (run B), where 2.46 fb^{-1} of luminosity was recorded. The MMT volumes containing dyon candidates were rescanned several times. For each candidate, it was found that the majority of the pole strengths measured were below the threshold of $0.4g_D$.

The maximum probability for missing a dyon in a single measurement was found to be 0.53% for a charge of $\pm 1g_D$. As two passes were made for each sample during run A (2015–2017), we have the negligible probability of missing the dyon twice of 0.0028%. Also, in run-A data, it was found that candidate events were associated with greater than average fluctuations in the SQUID signal. In this case, the probability of missing a dyon candidate was determined, using the 87 candidate events in run A, to be 0.2%. These probabilities become smaller with increasing magnetic charge. A more detailed description of the estimation of these probabilities is given in Supplemental Material [41]. In order to make a conservative estimate, we did not use the run-B data to assess the probability of missing a dyon.

We define the acceptance for the MMT detector to be the fraction of the number of events in which at least one dyon of the pair in an event was trapped in the MoEDAL trapping detector. The trapping condition is determined from the knowledge of the material traversed by the dyon [3,42] and the ionization energy loss of dyons when they go through matter [49–52], implemented in a simulation based on GEANT4 [53]. For a given dyon mass and charge, the pair-production model determines the kinematics and the overall trapping acceptance obtained. The uncertainty in the acceptance is dominated by uncertainties in the material description [3–5]. This contribution is estimated by performing simulations with hypothetical material conservatively added and removed from the nominal geometry model.

There are three causes of acceptance loss. The first is due to the limited geometrical extent of the MMT detector and the spin dependence in the geometrical acceptance due to

the different event kinematics. The second loss of acceptance is due to heavier, slower, dyons with smaller effective ionizing power punching through the trapping detector. We recall that in the case of magnetic charge the energy loss per unit distance falls with velocity. The third cause of acceptance loss is due to the dyon being absorbed in the material comprising the vertex locator detector, which encompasses the interaction point, before it reaches the MMT trapping volumes.

The largest acceptance is for dyons with spin 1 and magnetic charge $2g_D$ where, for mass up to $\sim 3 \text{ TeV}$ and electric charges up to $\sim 50e$, the acceptance is greater than or equal to 2.1%. The acceptance is below 0.1% over the whole mass range considered, for dyons that carry a magnetic charge of $6g_D$ or greater, for all values of electric charge. The maximum dyon electric and magnetic charge to which this analysis is sensitive is $\sim 200e$ and $5g_D$, respectively.

The material encountered by particles within the acceptance of the MoEDAL, before they reach the MoEDAL detector, varies from 0.1 to eight radiation lengths (X_0) with an average of roughly $1.4X_0$. The dominant systematic uncertainty comes from the estimated amount of material in the GEANT4 geometry description, yielding a relative uncertainty of $\sim 10\%$ for $1g_D$ dyons [3]. This uncertainty increases with the magnetic and electric charge, reaching a point (at $6g_D$) where it is too large for the analysis to be meaningful for spin-0 and spin-1/2 dyons. But, limits can be placed for spin-1 dyons with magnetic charge $6g_D$ and electric charge from 1 to $50e$.

We calculate cross-section upper limits at 95% C.L. using as a benchmark a DY model for dyon and magnetic monopole production, assuming a β -independent coupling, for three spin hypotheses (0, 1/2, and 1), magnetic charge up to $5g_D$, and, in the dyon case, electric charge up to $200e$. These values mark the limit of the sensitivity of this search due to the absorption of higher charges in the material comprising LHCb’s vertex locator detector that lies between the IP and the MMT detector.

An example of the limit curves obtained for spin-1/2 dyons with charge $1g_D$ is shown in Fig. 2. The corresponding

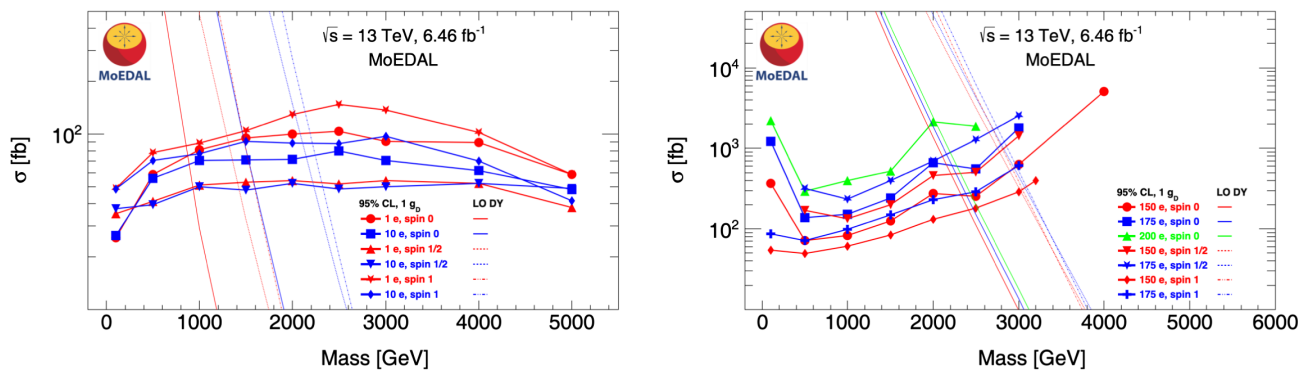


FIG. 2. Cross-section upper limits at 95% C.L. for DY spin-0, $-1/2$, and -1 dyon-pair production, with magnetic charge $1g_D$ and multiple electric charges, in 13 TeV pp collisions. The solid lines are leading-order cross-section calculations.

TABLE I. 95% C.L. mass limits found in a Drell-Yan production model for spin-0, spin-1/2, and spin-1 dyon-pair direct production in LHC pp collisions, assuming β -independent couplings.

Magnetic charge	Spin	Electric charge																	
		0	1	2	3	4	5	6	10	15	20	25	50	75	100	125	150	175	200
95% C.L. mass limits (GeV)																			
$1g_D$	0	870	870	980	1090	1180	1260	1320	1520	1700	1810	1910	2220	2320	2370	2370	2320	2210	2020
$2g_D$	0	1240	1160	1230	1310	1380	1440	1500	1680	1820	1920	2000	2210	2290	2320	2290	2210	2070	1950
$3g_D$	0	1300	1200	1240	1300	1350	1400	1450	1610	1740	1830	1910	2100	2170	2160	2090	2030
$4g_D$	0	1200	1080	1100	1150	1190	1230	1280	1420	1550	1630	1700	1870	1900	1920
$1g_D$	1/2	1400	1410	1580	1730	1840	1920	2000	2220	2410	2540	2640	2910	2970	2940	2840	2770	2700	...
$2g_D$	1/2	1810	1720	1810	1900	1990	2060	2120	2310	2470	2570	2670	2850	2870	2820	2740	2670
$3g_D$	1/2	1840	1720	1770	1830	1890	1940	2010	2180	2330	2440	2500	2670	2710	2660	2620	2510
$4g_D$	1/2	1680	1570	1580	1620	1660	1700	1740	1860	1970	2080	2210	2400	2480	2470	2390
$5g_D$	1/2	1460	1320	1340	1370	1390	1430	1480	1610	1740	1800	1890	2130
$1g_D$	1	1460	1460	1610	1730	1830	1910	1980	2210	2390	2540	2660	3000	3110	3120	3050	3030	2970	...
$2g_D$	1	1930	1840	1930	2020	2100	2170	2230	2410	2560	2670	2760	2990	3060	3040	2990	2930	2880	2770
$3g_D$	1	2040	1930	1980	2040	2100	2150	2200	2360	2490	2600	2680	2870	2930	2930	2880	2810
$4g_D$	1	1990	1870	1900	1930	1980	2020	2060	2210	2330	2420	2490	2680	2720	2770	2710
$5g_D$	1	1820	1700	1710	1740	1770	1810	1840	1960	2110	2200	2280	2480	2540	2510

limits for other dyons with spin 0, spin 1/2, and spin 1 and magnetic charges ranging up to and including $5g_D$ are given in Supplemental Material [41]. They are extracted on the basis of the acceptance estimates and their uncertainties; the delivered integrated luminosity 6.46 fb^{-1} , measured with a precision of 4% [54], corresponding to the full 2015–2018 exposure to 13 TeV pp collisions and the nonobservation of magnetic charge inside the trapping detector samples.

Using cross sections, computed at leading order, mass limits are obtained and reported in Table I. It is important to note that these DY cross sections are computed using perturbative field theory. However, the monopole-photon coupling is too large for such an approach. Thus, the mass limits given are only indicative.

Comparing the dyon mass limits with the corresponding monopole mass limits [6] obtained from the same dataset using an analog, we find, not surprisingly, that for the smallest electric charge of the dyon ($1e$) the limits obtained are comparable to or better than those obtained in the monopole search, as indicated in Table I.

In summary, we considered the direct production of dyon-antidyon pairs via the DY mechanism for the first time at an accelerator. The aluminum elements of the MoEDAL trapping detector exposed to 13 TeV LHC collisions during run 2 were scanned using a SQUID-based magnetometer to search for the presence of trapped magnetic charge belonging to dyons. No candidates survived our scanning procedure, and cross-section upper limits as low as 30 fb were set. As mentioned above, the trapping condition requires the dyon to be negatively electrically charged. Mass limits in the range

870–3120 GeV were set using a benchmark DY production model, for dyons with magnetic charge up to $5g_D$, for electric charge from $1e$ to $200e$, and for spins 0, 1/2, and 1. The corresponding mass limits for magnetic monopoles are in the range 870–2040 GeV for magnetic charges in the same range.

We note that many previous searches for highly ionizing particles would, in principle, also have sensitivity to dyons. However, no explicit search for dyons has ever been performed to date. We suggest that dyons be added to the list of highly ionizing particles for which dedicated searches are conducted at the LHC and at future colliders.

We thank CERN for the LHC’s successful run-2 operation, as well as the support staff from our institutions without whom MoEDAL could not be operated. We acknowledge the invaluable assistance of particular members of the LHCb Collaboration: G. Wilkinson, R. Lindner, E. Thomas, and G. Corti. Computing support was provided by the GridPP Collaboration, in particular, by the Queen Mary University of London and Liverpool grid sites. This work was supported by Grant No. PP00P2_150583 of the Swiss NSF; by the United Kingdom Science and Technology Facilities Council, via Grants No. ST/L000326/1, No. ST/L00044X/1, No. ST/N00101X/1, No. ST/P000258/1, and No. ST/T000759/1; by the Generalitat Valenciana via a special grant for MoEDAL and via the projects PROMETEO-II/2017/033 and PROMETEO/2019/087; by MCIU/AEI/FEDER, UE via Grants No. FPA2016-77177-C2-1-P, No. FPA2017-85985-P, No. FPA2017-84543-P, and No. PGC2018-094856-B-I00; by the Physics Department of King’s College London;

by NSERC via a project grant; by the V-P Research of the University of Alberta (UofA); by the Provost of the UofA; by UEFISCDI (Romania); by the INFN (Italy); by the Estonian Research Council via a Mobilitas Plus grant MOBTT5; by a National Science Foundation grant (United States) to the University of Alabama MoEDAL group; and by European Research Council, Grant No. MOBTT5.

*Deceased.

†Corresponding author.

jpinfold@ualberta.ca

‡Also at International Centre for Theoretical Physics, Trieste, Italy.

§Also at National Institute of Chemical Physics and Biophysics, Tallinn, Estonia.

||Also at Department of Physics, Faculty of Science, Beni-Suef University, Egypt.

¶Also at Physics Department, University of Regina, Regina, Saskatchewan, Canada.

**Also at Centre for Astronomy, Astrophysics and Geophysics, Algiers, Algeria.

- [1] P. A. M. Dirac, Quantised singularities in the electromagnetic field, *Proc. R. Soc. A* **133**, 60 (1931).
- [2] M. Tanabashi *et al.* (Particle Data Group), Review of particle physics, *Phys. Rev. D* **98**, 030001 (2019).
- [3] MoEDAL Collaboration, Search for magnetic monopoles with the MoEDAL prototype trapping detector in 8 TeV pp collisions at the LHC, *J. High Energy Phys.* **08** (2016) 067.
- [4] B. Acharya *et al.* (MoEDAL Collaboration), Search for Magnetic monopoles with the MoEDAL Forward Trapping Detector in 13 TeV pp Collisions at the LHC, *Phys. Rev. Lett.* **118**, 061801 (2017).
- [5] B. Acharya *et al.* (MoEDAL Collaboration), Search for magnetic monopoles with the MoEDAL forward trapping detector in 2.11 fb⁻¹ of 13 TeV pp collisions at the LHC, *Phys. Lett. B* **782**, 510 (2018).
- [6] B. Acharya *et al.* (MoEDAL Collaboration), Magnetic Monopole Search with the Full MoEDAL Trapping Detector in 13 TeV pp Collisions Interpreted in Photon-Fusion and Drell-Yan Production, *Phys. Rev. Lett.* **123**, 021802 (2019).
- [7] G. Aad *et al.* (ATLAS Collaboration), Search for Magnetic Monopoles in $\sqrt{s} = 7$ TeV pp Collisions with the ATLAS Detector, *Phys. Rev. Lett.* **109**, 261803 (2012).
- [8] G. Aad *et al.* (ATLAS Collaboration), Search for magnetic monopoles and stable particles with high electric charges in 8 TeV pp collisions with the ATLAS detector, *Phys. Rev. D* **93**, 052009 (2016).
- [9] G. Aad *et al.* (ATLAS Collaboration), Search for Magnetic Monopoles and Stable High-Electric-Charge Objects in 13 TeV pp Collisions with the ATLAS Detector, *Phys. Rev. Lett.* **124**, 031802 (2020).
- [10] S. Burdin, M. Fairbairn, P. Mermod, D. Milstead, J. Pinfold, T. Sloan, and W. Taylor, Non-collider searches for stable massive particles, *Phys. Rep.* **582**, 1 (2015).
- [11] L. Patrizii and M. Spurio, Status of searches for magnetic monopoles, *Annu. Rev. Nucl. Part. Sci.* **65**, 279 (2015).
- [12] N. E. Mavromatos and V. A. Mitsou, Magnetic monopoles revisited: Models and searches at colliders and in the cosmos, *Int. J. Mod. Phys. A* **35**, 2030012 (2020).
- [13] J. S. Schwinger, A magnetic model of matter, *Science* **165**, 757 (1969).
- [14] J. Goldstone and R. Jackiw, *Gauge Theories and Modern Field Theory*, edited by R. Arnowitt and P. Nath (MIT, Cambridge, MA, 1976), p. 377; E. Tomboulis and G. Woo, Soliton quantization in gauge theories, *Nucl. Phys.* **B107**, 221 (1976); P. Hasenfratz and D. Ross, Anomalous angular momenta in a quantized theory of monopoles, *Nucl. Phys.* **B108**, 462 (1976); N. Christ, A. Guth, and E. Weinberg, Canonical formalism for gauge theories with application to monopole solutions, *Nucl. Phys.* **B114**, 61 (1976).
- [15] E. Witten, Dyons of charge $e\theta/2\pi$, *Phys. Lett.* **86B**, 283 (1979).
- [16] See, e.g., Z.-q. Ma, Monopole and Dyon solutions in SU(5) unified gauge theory, *Nucl. Phys.* **B231**, 172 (1984); W. S. L'Yi, Y. J. Park, I. G. Koh, and Y. D. Kim, Analytic Dyon Solution In Su(n) Grand Unified Theories, *Phys. Rev. Lett.* **49**, 1229 (1982).
- [17] See, e.g., J. Bjoeraker and Y. Hosotani, Stable Monopole and Dyon Solutions in the Einstein-Yang-Mills Theory in Asymptotically Anti-De Sitter Space, *Phys. Rev. Lett.* **84**, 1853 (2000); B. Nolan and E. Winstanley, On the existence of dyons and dyonic black holes in Einstein-Yang-Mills theory, *Classical Quantum Gravity* **29**, 235024 (2012).
- [18] See, e.g., A. Sen, Kaluza-Klein Dyons in String Theory, *Phys. Rev. Lett.* **79**, 1619 (1997); Z.-M. Xi, Fermion interactions with A K-K Dyon, *Europhys. Lett.* **3**, 157 (1987).
- [19] See, e.g., A. Dabholkar, J. Gomes, and S. Murthy, Counting all dyons in $N = 4$ string theory, *J. High Energy Phys.* **05** (2011) 059.
- [20] See, e.g., C. Gomez and J. J. Manjarin, Dyons, K theory and M theory, [arXiv:hep-th/0111169](https://arxiv.org/abs/hep-th/0111169).
- [21] Y. M. Cho, Physical implications of an electroweak monopole, *Phil. Trans. R. Soc. A* **377**, 20190038 (2019).
- [22] P. Q. Hung, Topologically stable, finite-energy electroweak-scale monopoles, *Nucl. Phys.* **B962**, 115278 (2021).
- [23] J. Alexandre and N. E. Mavromatos, Weak-U(1) x strong-U(1) effective gauge field theories and electron-monopole scattering, *Phys. Rev. D* **100**, 096005 (2019).
- [24] N. E. Mavromatos and S. Sarkar, Finite-energy dressed string-inspired Dirac-like monopoles, *Universe* **5**, 8 (2018).
- [25] J. Ellis, N. E. Mavromatos, and T. You, The price of an electroweak monopole, *Phys. Lett. B* **756**, 29 (2016).
- [26] A. Dainese *et al.*, Report on the physics at the HL-LHC, and perspectives for the HE-LHC, CERN Report No. CERN-2019-007, 2019, p. 1418, <https://doi.org/10.23731/CYRM-2019-007>.
- [27] B. Holdom, J. Ren, and C. Zhang, Quark Matter May Not Be Strange, *Phys. Rev. Lett.* **120**, 222001 (2018).
- [28] E. Farhi and R. L. Jaffe, Strange matter, *Phys. Rev. D* **30**, 2379 (1984).
- [29] S. Coleman, Q-balls, *Nucl. Phys.* **B262**, 263 (1985).
- [30] A. Kusenko and M. E. Shaposhnikov, Supersymmetric Q-balls as dark matter, *Phys. Lett. B* **418**, 46 (1998).
- [31] B. Koch, M. Bleicher, and H. Stöcker, Black holes at the LHC?, *J. Phys. G* **34**, S535 (2007).

- [32] G. Aad *et al.* (ATLAS Collaboration), Search for massive long-lived highly ionising particles with the ATLAS detector at the LHC, *Phys. Lett. B* **698**, 353 (2011).
- [33] M. Fairbairn, A. C. Kraan, D. A. Milstead, T. Sjöstrand, P. Skands, and T. Sloan, Stable massive particles at colliders, *Phys. Rep.* **438**, 1 (2007).
- [34] In the search for HECOs, one must consider the possibility of screening due to vacuum pair production via the Schwinger mechanism in the case of high electric charges. As argued in Ref. [35], screening can affect the results for electric charges higher than 500, due to the strong electric fields produced in such cases. However, this issue does not arise for the range of electric and magnetic charges of the dyon discussed in this work.
- [35] C. Englert and J. Jaeckel, Getting stuck! Using monosignatures to test highly ionizing particles, *Phys. Lett. B* **769**, 513 (2017).
- [36] J. Alwall, R. Frederix, S. Frixione, V. Hirschi, F. Maltoni, O. Mattelaer, H.-S. Shao, T. Stelzer, P. Torrielli, and M. Zaro, The automated computation of tree-level and NLO differential cross sections, and their matching to parton shower simulations, *J. High Energy Phys.* **07** (2014) 079.
- [37] S. Baines, N. E. Mavromatos, V. A. Mitsou, J. L. Pinfold, and A. Santra, Monopole production via photon fusion and Drell-Yan processes, *Eur. Phys. J. C* **78**, 966 (2018); Erratum, *Eur. Phys. J. C* **79**, 166 (2019).
- [38] R. D. Ball *et al.* (NNPDF Collaboration), Parton distributions with LHC data, *Nucl. Phys.* **B867**, 244 (2013).
- [39] L. P. Gamberg and K. A. Milton, Dual quantum electrodynamics: Dyon-dyon and charge monopole scattering in a high-energy approx, *Phys. Rev. D* **61**, 075013 (2000).
- [40] L. P. Gamberg and K. A. Milton, Eikonal scattering of monopoles and dyons in dual QED, [arXiv:hep-ph/0005016](https://arxiv.org/abs/hep-ph/0005016).
- [41] See Supplemental Material at <http://link.aps.org/supplemental/10.1103/PhysRevLett.126.071801> for more detailed description of the MoEDAL detector; extra information on the determination of the probability of a false negative in the search for magnetic charge; and, plots of the cross-section upper limits at 95% C.L. for dyon pair production for all dyon charge (electric and magnetic) and spin assignments considered.
- [42] A. A. Alves *et al.* (LHCb Collaboration), The LHCb Detector at the LHC, *J. Instrum.* **3**, S08005 (2008).
- [43] J. L. Pinfold, The MoEDAL experiment: A new light on the high-energy frontier, *Phil. Trans. R. Soc. A* **377**, 20190382 (2019).
- [44] L. P. Gamberg, G. R. Kalbfleisch, and K. A. Milton, Direct and indirect searches for low mass magnetic monopoles, *Found. Phys.* **30**, 543 (2000).
- [45] C. J. Goebel, Binding of nuclei to monopoles, in *Monopole '83*, edited by J. L. Stone (Plenum, New York, 1984), p. 333.
- [46] L. Bracci and G. Fiorentini, Interactions of magnetic monopoles with nuclei and atoms, *Nucl. Phys.* **B232**, 236 (1984).
- [47] K. Olaussen and R. Sollie, Form-factor effects on nucleus-magnetic monopole binding, *Nucl. Phys.* **B255**, 465 (1985).
- [48] A. De Roeck, H.-P. Hächler, A. M. Hirt, M.-D. Joergensen, A. Katre, P. Mermod, D. Milstead, and T. Sloan, Development of a magnetometer-based search strategy for stopped monopoles at the large hadron collider, *Eur. Phys. J. C* **72**, 2212 (2012).
- [49] S. P. Ahlen, Stopping-power formula for magnetic monopoles, *Phys. Rev. D* **17**, 229 (1978).
- [50] S. P. Ahlen, Theoretical and experimental aspects of the energy loss of relativistic heavily ionizing particles, *Rev. Mod. Phys.* **52**, 121 (1980); Erratum, *Rev. Mod. Phys.* **52**, 653 (1980).
- [51] S. P. Ahlen and K. Kinoshita, Calculation of the stopping power of very-low-velocity magnetic monopoles, *Phys. Rev. D* **26**, 2347 (1982).
- [52] S. Cecchini, L. Patrizii, Z. Sahnoun, G. Sirri, and V. Togo, Energy losses of magnetic monopoles in Al, Fe and Cu, [arXiv:1606.01220](https://arxiv.org/abs/1606.01220).
- [53] J. Alison *et al.* (GEANT4 Collaboration), Geant-4 developments and apps, *IEEE Trans. Nucl. Sci.* **53**, 270 (2006).
- [54] R. Aaij *et al.* (LHCb Collaboration), Measurement of the inelastic pp cross-section at $\sqrt{s} = 13$ TeV, *J. High Energy Phys.* **06** (2018) 100.